Diffuse phase transition of barium-substituted lead-ytterbium-niobate ceramics

1992 J. Phys.: Condens. Matter 4 2309

(http://iopscience.iop.org/0953-8984/4/9/024)

J. Phys.: Condens. Matter 4 (1992) 2309–2321. Printed in the UK

Diffuse phase transition of barium-substituted lead–ytterbium–niobate ceramics

Woong-Kil Choo and Hyo-Jin Kim
Department of Materials Science and Engineering, Korea Advanced Institute of Science and Technology, PO Box 150, Cheongryang, Seoul, Korea

Received 3 July 1991, in final form 22 October 1991

Abstract. The behaviour of the diffuse phase transition of $(Pb_{1-x}Ba_x)(Yb_{1/2}Nb_{1/2})O_3$ $(0 \leq x \leq 0.3)$ ceramics has been investigated with special attention to the phase boundary near $x = 0.12$. The temperature and frequency dependence of the dielectric constant ε and loss tan δ have been carefully measured together with heat capacity measurements. Above $x = 0.12$, the phase transition is broadened and frequency dependent, while the AFE-PE phase transition is sharp and ε closely follows the Curie–Weiss law above T_N for $0 \leq x < 0.1$. Also, above $x = 0.12$, $(1/\varepsilon - 1/\varepsilon_m)$ is proportional to $(T - T_t)^n$ at $T > T_t$, where ε_m is the peak value of ε at T_t and n is an exponent. The value of n is dramatically increased for $0.1 \leq x \leq 0.14$, and then increased linearly with increasing Ba-content $(dn/dx = 1.78 \times 10^{-2}\,\%^{-1})$ for $0.14 \leq x \leq 0.3$. T_N decreases markedly for $0 \leq x < 0.12$, whereas the value of T_t is reduced linearly with increasing x-value $(dT_t/dx = -6.61\,°C\%^{-1})$ for $0.14 \leq x \leq 0.3$. Another remarkable feature is an anomalous enhancement of ε_m between $x = 0.1$ and $x = 0.14$. Heat capacity measurements have revealed a well-defined anomaly associated with the AFE-PE transition, increasingly broadening with Ba-content for $0 \leq x < 0.1$. For $0.1 \leq x \leq 0.14$, the heat capacity anomaly is extremely broadened and a small deviation from the extrapolated baseline can be seen. In particular, we cannot detect any heat capacity anomaly associated with T_t above $x = 0.14$, which is suggested as additional evidence for DPT. These salient features are discussed in the light of the formation of locally ordered polar microdomains within a non-polar matrix and the pseudo-cubic structure above $x = 0.12$.

1. Introduction

A great deal of attention has been given to ferroelectrics with diffuse phase transition (DPT) because of their high application potential. The mechanism of DPT has not been fully clarified despite a number of theoretical and experimental works [1–12]. DPT is usually explained by the presence of dipole inhomogeneity. The inhomogeneity is either ascribed firstly to the composition fluctuation [1] which is almost macroscopic in scale, secondly to the fluctuation in chemical ordering [5, 6] which is intermediate in length scale, and thirdly to the glassy dipolar arrangement [7–9] whose scale is of the order of lattice parameters. More recently, solute-deficient regions of a PLZT perovskite solid solution have been ascribed to the onset of local polarization in DPT ferroelectrics [10]. Another DPT mechanism operating in $Pb(Sc_{1/2}Nb_{1/2})O_3$ has been assigned to the kinetic process leading to the Känzig domain formation [11]. In general, DPT is observed with

0953-8984/92/092309 + 13 $04.50

virtually no exceptions in solid solutions [1, 8, 10, 12] and in disordered crystalline perovskites [11, 13, 14].

It is well known that cation ordering, or lack of it, is closely related to diffuse phase transitions [1, 2, 6, 8, 11, 15]. When ordered, the complex perovskite displays a sharp phase transition of the first-order type from a paraelectric (PE) to ferroelectric (FE) (or antiferroelectric—AFE) phase [6, 15, 16]. Lead ytterbium niobate, $Pb(Yb_{1/2}Nb_{1/2})O_3$, is antiferroelectric with an ordered perovskite-type structure which manifests itself by displaying prominent B-site cation ordering [17, 18]. In the mean time, the low temperature superlattice structure of PYN that originates from the structural phase transition has only been revealed recently [16]. The phase transition from a cubic PE phase with space group $Fm3m$–O_h^5 to an orthorhombic AFE phase with space group $Pbnm$–D_{2h}^{16} has been proposed based on x-ray diffraction and transmission electron microscopy investigations.

In a recent study [19], the temperature dependence of the structure of barium substituted lead ytterbium niobate $(Pb_{1-x}Ba_x)(Yb_{1/2}Nb_{1/2})O_3$ $(0 \leqslant x \leqslant 0.3)$ was investigated by x-ray powder diffraction analysis. It has been revealed that the high temperature phase of $(Pb_{1-x}Ba_x)(Yb_{1/2}Nb_{1/2})O_3$, for all compositions studied, is still a B-site ordered perovskite type of space group $Fm3m$–O_h^5 with the doubled perovskite unit cell, which is characterized by the presence of superlattice peaks ascribed to the ordering of Yb^{3+} and Nb^{5+} ions. Near $x = 0.12$, the low symmetry phase changes from an orthorhombic to a pseudo-cubic phase with increasing Ba concentration. The diminution of orthorhombic distortion in the low temperature phase was accompanied by the absence of superlattice peaks that originated from the AFE displacement mode beyond $x = 0.12$. From a structural standpoint, it was proposed that the dielectric phase changes from the AFE to the FE state near $x = 0.12$. In this work, this suggestion will be supported by the observation of ferroelectric P-E hysteresis loops above $x = 0.10$. As will be seen later, the AFE-PE phase transition is relatively sharp, but the FE-PE phase transition is diffuse. Our prime concern in this study is to elucidate the nature of DPT in the $(Pb_{1-x}Ba_x)(Yb_{1/2}Nb_{1/2})O_3$ system, focusing our attention on the effect of barium substitution.

In the present work, we have performed experiments to determine the temperature and frequency dependence of the dielectric constant and dielectric loss tangent in the A-site substituted $(Pb_{1-x}Ba_x)(Yb_{1/2}Nb_{1/2})O_3$ $(0 \leqslant x \leqslant 0.3)$ ceramics system. In order to examine the ferroelectricity, P-E hysteresis curves have been inspected. Heat capacity behaviour has also been investigated in the temperature range around the phase transition temperature. We will also present several salient features associated with the different types of phase transition in this system. In reference to the crystal structure study [19], we will further show via the dielectric study that the orthorhombic–pseudo-cubic phase boundary lies in the vicinity of $x = 0.12$ and thus infer that a possible miscibility gap exists between $x = 0.1$ and $x = 0.14$. Furthermore, we will discuss the nature of the phase transitions of $(Pb_{1-x}Ba_x)(Yb_{1/2}Nb_{1/2})O_3$ $(0 \leqslant x \leqslant 0.3)$ in terms of the general picture of DPT behaviour and the presence of a pseudo-cubic structure for $x \geqslant 0.12$.

2. Experimental procedure

The ceramic compacts of formula $(Pb_{1-x}Ba_x)(Yb_{1/2}Nb_{1/2})O_3$ $(0 \leqslant x \leqslant 0.3)$ were prepared by reacting stoichiometric proportions of PbO, Yb_2O_3, Nb_2O_5 and $BaCO_3$ species

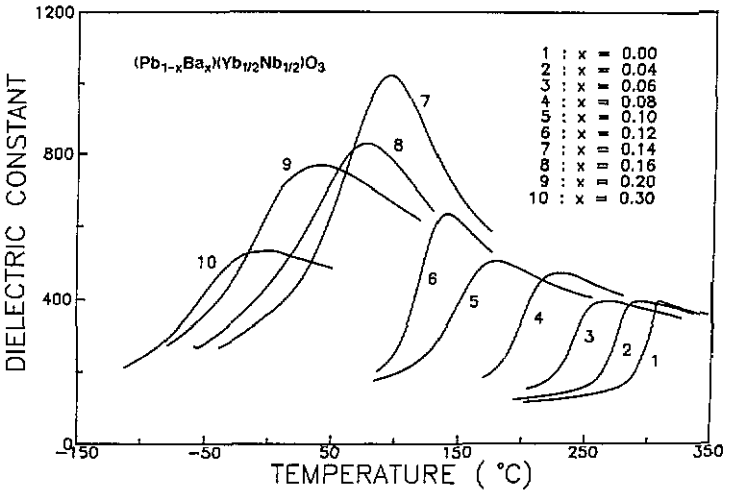

Figure 1. Temperature dependence of the dielectric constant ε at 1 kHz on heating in the $(Pb_{1-x}Ba_x)(Yb_{1/2}Nb_{1/2})O_3$ $(0 \leq x \leq 0.3)$ system with variation of Ba concentration x.

using high-purity (99.9%) grade chemicals. The mixtures were ball-milled in acetone, dried, and then calcinated at 900–1000 °C for 2 h. The calcinated powders were reground, and pressed into discs of diameter 14 mm and thickness 2–3 mm. The discs were sintered at 1120–1350 °C for 1 h in a controlled PbO atmosphere in order to prevent the loss of PbO. Sintered specimens were cut with a diamond wafering saw and polished to the final thickness of 0.4–0.6 mm. No second phase has been observed in x-ray diffraction. The apparent densities of ceramic compacts were about 95% of the respective theoretical densities. Then, the specimens for dielectric investigations were electroded with silver paste (Dupont No 7075) by firing at 590 °C for 5 min.

The electrical capacitance and the dielectric loss tangent were measured at several frequencies, between 1 kHz and 1 MHz, using a Hewlett-Packard 4194A Impedance/Gain-Phase Analyser interfaced with a IBM PC/AT, while the sample was heated at a constant rate of 2 °C min^{-1}. Its temperature was monitored by a copper–constantan thermocouple through a Fluke 2190A Digital Thermometer to an accuracy of ±0.5 °C. Measured capacitance and sample dimensions were used to calculate the relative dielectric constant ε. Using a Sawyer–Tower circuit, the P-E hysteresis curves were observed at room temperature under AC field with an amplitude of 10 kV cm^{-1} and 60 Hz.

Heat capacities of specimens with differing Ba concentrations were obtained in the temperature range around the transition temperature using a Perkin Elmer DSC7 Differential Scanning Calorimeter. The heating rate was maintained at 10 °C min^{-1}. The latent heat of transition for each sample was calculated by extrapolating a base line from the region outside the transition range and by determining the area between this extrapolated base line and the measured thermal curve.

3. Experimental results and discussion

3.1. Dielectric properties

Figure 1 shows the temperature dependence of the dielectric constant ε of the $(Pb_{1-x}Ba_x)(Yb_{1/2}Nb_{1/2})O_3$ $(0 \leq x \leq 0.3)$ ceramics system at 1 kHz on heating for a

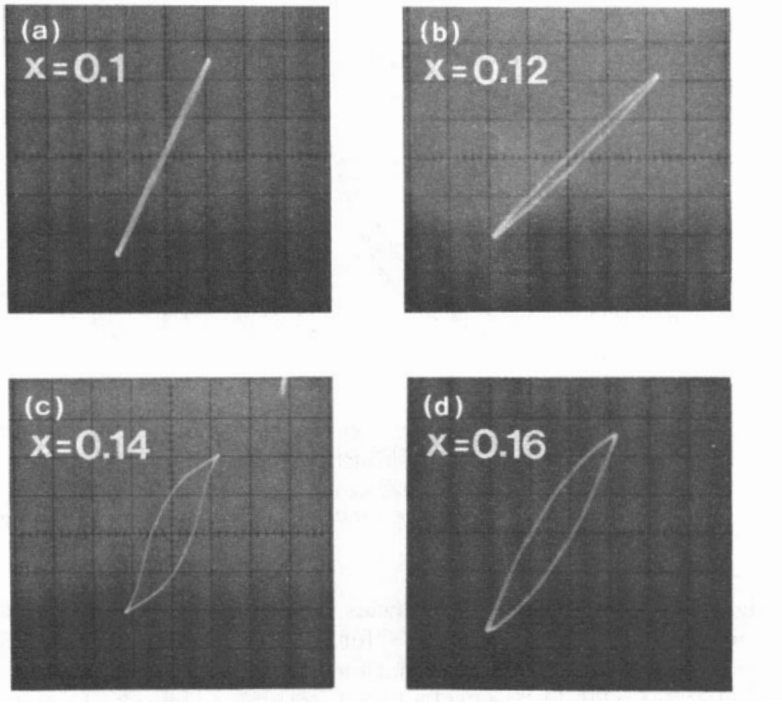

Figure 2. P–E hysteresis curves at room temperature in the vicinity of the phase boundary of the $(Pb_{1-x}Ba_x)(Yb_{1/2}Nb_{1/2})O_3$ system. An AC field with an amplitude of 10 kV cm^{-1} and 60 Hz is applied.

series of different Ba concentrations. In the case of pure $Pb(Yb_{1/2}Nb_{1/2})O_3$ ($x = 0$), the temperature dependence of ε follows exactly the Curie–Weiss law above the AFE phase transition temperature $T_N = 308$ °C on heating, and 302 °C on cooling. The thermal hysteresis indicates that the PE–AFE transition is first-order. For $0 < x \leq 0.1$, the temperature dependence of ε faithfully follows the Curie–Weiss law above T_N, and its general appearance is similar to that of pure $Pb(Yb_{1/2}Nb_{1/2})O_3$. For $x > 0.12$, the general appearance of the dielectric constant versus temperature curve is distinctly different from that of the lower concentration range. Broad maxima are observed in the ε versus T curves at the apparent transition temperature T_t. The broadening increases with increasing Ba concentration, while the transition temperature continues to decrease. As will be seen in what follows, the dielectric constant closely obeys the Curie–Weiss law above a temperature designated as T_{CW} but deviates significantly from the Curie–Weiss law below T_{CW}.

Figure 2 shows the P–E hysteresis curves observed at room temperature in the vicinity of the structural phase boundary of the $(Pb_{1-x}Ba_x)(Yb_{1/2}Nb_{1/2})O_3$ system. For $x \geq 0.12$, ferroelectric hysteresis loops are clearly seen. The calculated spontaneous polarizations, P_s, are 4.24, 10.23 and 6.0 μC cm^{-2} for $x = 0.12$, 0.14 and 0.16, respectively. In connection with structural change [19], it is consequently concluded that the low temperature phase changes from an orthorhombic AFE to a pseudo-cubic FE phase near $x = 0.12$ with increasing Ba concentration. Then, the significant change of the general appearance of the ε versus T curves above $x = 0.1$ can be partly related to the onset of ferroelectricity.

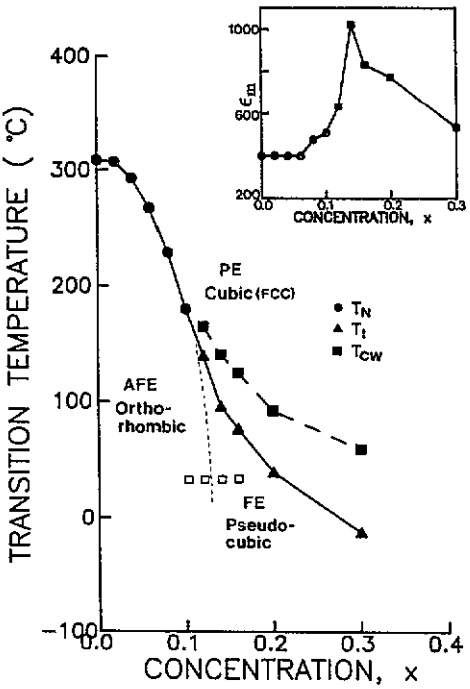

Figure 3. Phase diagram of $(Pb_{1-x}Ba_x)(Yb_{1/2}Nb_{1/2})O_3$ $(0 \leq x \leq 0.3)$ determined from the dielectric measurements. The squares denote where the P–E hysteresis curves in figure 2 have been observed. The dotted curve indicates a hypothetical phase boundary. The inset shows the concentration dependence of the maximum value of dielectric constant ε_m.

Figure 3 shows the phase diagram of $(Pb_{1-x}Ba_x)(Yb_{1/2}Nb_{1/2})O_3$ $(0 \leq x \leq 0.3)$ determined from the dielectric measurements. Also, the concentration dependence of the maximum value ε_m of the dielectric constant at 1 kHz is shown in the inset. It is found that T_N defined for $0 < x < 0.12$ decreases rapidly, whereas T_t defined for $0.14 < x < 0.3$ decreases more slowly with increasing Ba concentration at a rate of $dT_t/dx \approx -6.61\,°C\,mol\%^{-1}$. Another prominent feature to be pointed out here is the anomalous growth of the dielectric constant between $x = 0.1$ and $x = 0.14$. Obviously, the change in the transition characteristics as a function of Ba concentration and the anomalous dielectric constant growth are closely connected with the evolution from the PE–AFE to PE–FE phase change marked near $x = 0.12$. The latter fact will be addressed later in terms of a proposed model to elucidate the nature of DPT in our system.

The frequency dependence of the dielectric constant and loss tangent as a function of temperature for $x = 0.20$ is shown in figure 4(*a*). Both large broadening and a shift toward higher temperatures in the dielectric constant versus temperature curve take place. The temperature of the maximum dielectric constant changes at a rate of $dT_t/d\ln\omega = 5.7\,°C$ between 1 and 1000 kHz as contrasted with no such shift in the dielectric constant curves of pure $Pb(Yb_{1/2}Nb_{1/2})O_3$ as shown in the inset in figure 4(*a*). Also, the dielectric loss tangent shows a peak which shifts toward the higher temperature side with increasing frequency, but its peak occurs at a temperature different from the maximum in the real part of the dielectric constant. This typical relaxor behaviour, a manifestation of DPT phenomena, has been observed for all samples for $x \geq 0.12$ as shown by three other examples in figure 4(*b*). The frequency dependency of T_t becomes more apparent with increasing Ba concentration.

The experimental results which have been discussed so far can be interpreted if we take into account the fact that there exists a considerable perturbation which can be

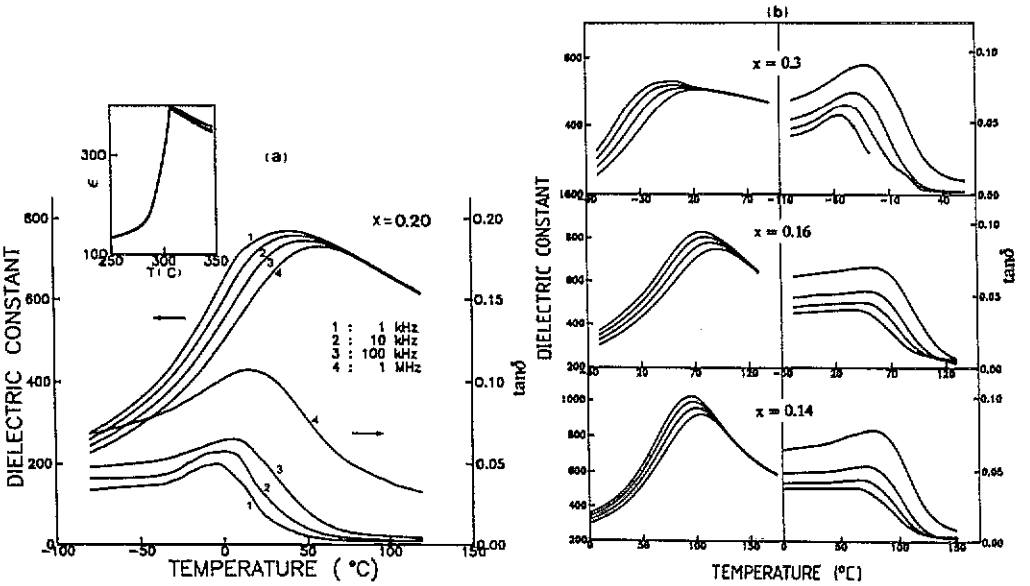

Figure 4. Temperature dependence of the dielectric constant ε and the loss tangent tan δ at different frequencies for (*a*) $x = 0.2$, and (*b*) three other examples showing DPT. In (*b*) the four curves in each part from upper to lower show dependencies at frequency of 1 kHz, 10 kHz, 100 kHz and 1 MHz, respectively. The inset in (*a*) shows the case of pure $Pb(Yb_{1/2}Nb_{1/2})O_3$.

pictured as an inevitable change in the local dipole configuration induced by substituted barium ions. The dipole distribution is a dynamical rather than a static one. The experimental data of relative dielectric constant ε of most DPT ferroelectrics in the vicinity of the apparent transition can be successfully fitted by a semi-empirical equation of the form [12, 20, 21]

$$1/\varepsilon - 1/\varepsilon_m = (T - T_t)^n/A \tag{1}$$

where ε_m is the maximum dielectric constant at the apparent transition temperature, A is a constant, and n is a critical exponent varying between 1 and 2. Exponent n is 1 when the transition is of the Curie–Weiss type, while it is considered to be 2 if the transition is a complete DPT. Equation (1) with $n = 2$ was originally used to describe the dielectric constant behaviour of DPT ferroelectrics [1, 22].

Equation (1) may be rewritten in a dimensionless form as

$$(\varepsilon_m - \varepsilon)/\varepsilon = (T_t/\sigma)^n(T/T_t - 1)^n \tag{2}$$

where σ may now be considered as a parameter showing the degree of thermal diffuseness or it has a clear physical meaning when $n = 1$. In this case σ is the Curie–Weiss constant. In case $n = 2$, the distribution of the polar regions may be assumed as a function of temperature in a Gaussian form, and σ^2 is defined as the mean square thermal deviation [1, 22]. Exponent n can be readily determined from the slope of the log–log plot of (2), and σ can be estimated from the y-axis intercept of the same plot using the predetermined value of n and the measured value of ε_m.

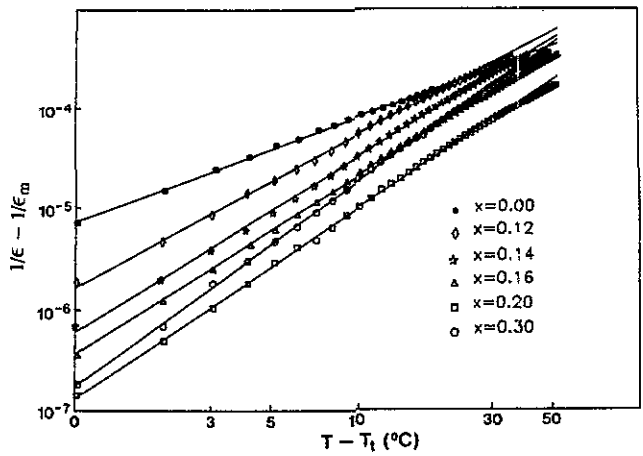

Figure 5. Logarithmic plots of the reciprocal dielectric constant $(1/\varepsilon - 1/\varepsilon_m)$ at 1 kHz against the reduced temperature $(T - T_t)$ for $(Pb_{1-x}Ba_x)(Yb_{1/2}Nb_{1/2})O_3$ $(0 \leqslant x \leqslant 0.3)$ showing DPT. For the sake of comparison, the same type of plot is drawn for pure $Pb(Yb_{1/2}Nb_{1/2})O_3$.

Figure 5 shows the logarithmic plots of the reciprocal dielectric constant $(1/\varepsilon - 1/\varepsilon_m)$ at 1 kHz versus the reduced temperature $(T - T_t)$ for some of the samples showing DPT. For comparison, the same plot for pure $Pb(Yb_{1/2}Nb_{1/2})O_3$, which exactly follows the Curie–Weiss law, is drawn. The values of exponent n have been determined by measuring the slope in the temperature range where the experimental data show unambiguously straight-line behaviour. It can be clearly seen that n increases with increasing Ba concentration. Note that at higher temperatures, for example $(T - T_t) > 32$ for $x = 0.14$ and $(T - T_t) > 44$ for $x = 0.2$, the temperature dependence of the dielectric constant follows the Curie–Weiss law. A similar dependency was observed at temperatures higher than T_{CW} in $(Pb_{1-3x/2}La_x)(Zr_{1-y}Ti_y)O_3$ (PLZT) [15], $Pb(Mg_{1/3}Nb_{2/3})O_3$ [23] and $Pb(Fe_{1/2}Nb_{1/2})O_3$ [14] etc. Uchino and Nomura [20] and Choo and Lee [12] indicated that $A(B'_xB''_{1-x})O_3$ ferroelectrics obey the Curie–Weiss law $(1/\varepsilon - 1/\varepsilon_m) \propto (T - T_t)$ for $(T - T_t) \gg \sigma'$ where σ' is a measure of the DPT range. In a way, we may equate $(T_{CW} - T_t)$ to σ', T_{CW} being the temperature above which the dielectric constant as a function of temperature follows the Curie–Weiss law [15]. Such experimental values of T_{CW} and $(T_{CW} - T_t)$ are shown in figure 3.

Figure 6 shows the experimentally determined n and σ values. The n values were obtained from the slopes of figure 4, and the σ values were obtained from the y-axis intercepts of the same plots. One distinct feature to be pointed out is the fact that both the slopes of the n and σ values versus temperature change pronouncedly between $x = 0.1$ and $x = 0.14$, and then further slow down with increasing Ba concentration. At $x = 0.3$, the value of n approaches 2 to manifest a complete DPT, and the magnitude of σ is found to be 63 °C.

The noticeable increase in measures of DPT may be interpreted in conjunction with the AFE–FE phase coexistence. This assumption is partially based on the fact that $(Pb_{1-x}Ba_x)(Yb_{1/2}Nb_{1/2})O_3$ for $x \geqslant 0.12$ displays a P–E hysteresis loop at room temperature although no such loop is detected for $x \leqslant 0.10$. In the intervening Ba composition region, the phase transition can be pictured as a simultaneous appearance of AFE and FE microdomains or 'polar microdomains' with local crystal structures different

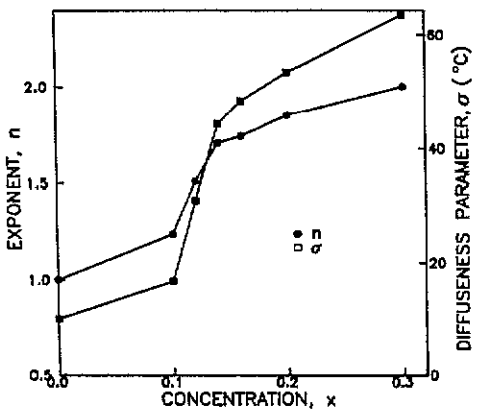

Figure 6. Concentration dependence of the exponent n and the diffuseness parameter σ in the $(Pb_{1-x}Ba_x)(Yb_{1/2}Nb_{1/2})O_3$ $(0 \leq x \leq 0.3)$ system.

from one another among the PE matrix. A local structural transition spread throughout the crystal may become possible due to the presence of different local atomic vibrations which in turn are dependent on each local atom environment created by the local configuration and the concentration fluctuation of solute Ba^{2+} ions. Moreover, such microregions, especially polar microdomains, are isolated from one another at temperatures well above $T_t(x)$ where x is the average concentration of Ba^{2+} ions, since $T_t(x)$ decreases rapidly with increasing Ba concentration. Consequently, there exist highly-localized short-range dipolar domains and microscopic structural fluctuations of strength, which lead to an abrupt increase of the intensity of DPT. It is reminded herein that the broadening of the phase transition of PLZT becomes pronounced at high La concentrations [15]. The same trend was also observed near the morphotropic phase boundary (MPB) of $(Pb_{1-x}Ba_x)(Zr_{1-y}Ti_y)O_3$ [24].

Before the more detailed analysis of DPT in $(Pb_{1-x}Ba_x)(Yb_{1/2}Nb_{1/2})O_3$, we would like to address the anomalous growth of the dielectric maxima in the boundary composition band $0.10 < x \leq 0.14$, as shown in the inset in figure 2. Indeed, the dielectric constant maximum value achieves its largest value at $x = 0.14$, and decreases with increasing Ba concentration. Such an abrupt dielectric constant jump is a well-established phenomenon of $Pb(Zr_{1-x}Ti_x)O_3$ (PZT) at MPB. In analogy with what happens at MPB in PZT, we conjecture that the anomalous increase of dielectric constant in our system is traced to the orthorhombic and pseudo-cubic (possibly rhombohedral) phase coexistence at the phase boundary. Hence, the phase boundary can be indeed redefined as the centre of the phase boundary band in which two phases coexist. Actually in our two-phase mixture assumption, the spontaneous polarization P_s of each polar microdomain is reckoned to be randomly orientated and thus can be rotated by thermal agitation since the low-temperature FE structure is nearly cubic or pseudo-cubic. Under the circumstances, each localized polarization requires only a small BO_6 octahedral distortion to become polarized. A dipole moment μ can contribute additional $\varepsilon_{rot} \propto \mu^2 k_B T$ to the dielectric constant according to Langevin's theory [25].

The increasing tendency of $(Pb_{1-x}Ba_x)(Yb_{1/2}Nb_{1/2})O_3$ to become polar with increasing Ba concentration may be ascribed to the ionic radius difference between Ba^{2+} (1.38 Å) and Pb^{2+} (1.26 Å), which leads to the expansion of the unit cell volume with increasing Ba concentration [19]. According to Migoni *et al* [26], the driving factor of ferroelectricity in perovskite oxides (ABO_3) is the oxygen polarizability along the O–B chain, which is strongly dependent on the surroundings [27]. The electrical polarizability

of the O^{2-} ion increases with an increase of the volume which it occupies [27]. In perovskite, the dimension of the O^{2-} ion relative to the O–B distance increases with increasing A-site ionic radius and decreasing B-site ionic radius. Consequently, the ionic radius of O^{2-} increases with increasing Ba concentration in our system. This leads to an increase of the oxygen polarizability and so facilitates the instability of the ferroelectric mode. In brief, the onset of ferroelectricity originates from the change of the nature of chemical bonds associated with volume expansion due to Ba substitution. The revealed diffuse nature of the PE-FE phase transition indicates that the FE order parameter correlation length is short-range, forming small disconnected clusters of electrically polarized material.

From the structural standpoint, the AFE phase in low Ba concentration is orthorhombic and the FE phase in high Ba concentration is pseudo-cubic. Because of the Ba^{2+} and Pb^{2+} size difference, short range strain fields may well be developed in the analogous manner as in the orientation order parameter–random strain coupling in the mixed crystal $K(CN)_yBr_{1-y}$ [28]. In the $K(CN)_yBr_{1-y}$ system, the CN^- and Br^- size difference and the concentration y play an important role in determining the phase diagram. The low temperature phase of high y was defined to be 'orientationally glassy' while that of low y, orthorhombic. In fact, we find that the outlooks of the two phase diagrams are quite similar. Hence, we may designate the high x and thus pseudo-cubic phase as a disordered polar phase if not glassy.

In view of theoretical descriptions [29, 30] of the phenomena observed in $Li_xK_{1-x}TaO_3$ on the line of spin glass models [31], the creation of local dipole moments [32] at the Pb site is ascribed to the ionic size misfit. Random interactions between these moments display the effects of the polarizable lattice, as simulated in an NaCl lattice by Wang [33]. The random-interaction theory (spin glass models) predicts that the interacting species show a dielectric response which is broadened with respect to the Debye response. Consequently, a close investigation of the dielectric relaxation by means of direct comparison of experimental with model parameters will provide more physical insight into the nature of DPT in our system. This type of work [34, 35], in general, needs dielectric response data over a wide range of frequency. Further investigation on the dielectric relaxation phenomena for DPT, including the growth of single crystals, is in progress.

3.2. Thermal properties

Figure 7 shows the temperature dependence of heat capacity of pure $Pb(Yb_{1/2}Nb_{1/2})O_3$ which was measured on heating. A sharp decrease of the heat capacity just above T_N = 308 °C is observed and a short plateau takes place below T_N. This fact is consistent with the dielectric constant (see figure 1) and further confirms the fact that the AFE–PE phase transition is of first-order. The calculated values of the heat of transition ΔH and the entropy change ΔS are 832 J mol^{-1} and 1.42 J K^{-1} mol^{-1}, respectively. This ΔH value is quite comparable to ΔH = 840 J mol^{-1} of $Pb(Co_{1/2}W_{1/2})O_3$ [36] also with an ordered perovskite structure.

Figure 8 shows the variation in transition temperature with Ba concentrations displayed by the heat capacity of $(Pb_{1-x}Ba_x)(Yb_{1/2}Nb_{1/2})O_3$. For $0 < x < 0.1$, well-defined heat capacity anomalies are manifested. The transition temperature defined by the heat capacity maximum follows rather closely the AFE transition temperature T_N change as a function of the Ba concentration as shown in figure 3. The heat capacity anomaly becomes rapidly broadened with increasing Ba concentration and at the same time the

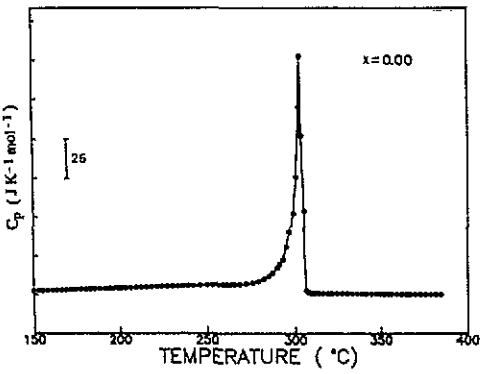

Figure 7. Heat capacity of pure $Pb(Yb_{1/2}Nb_{1/2})O_3$.

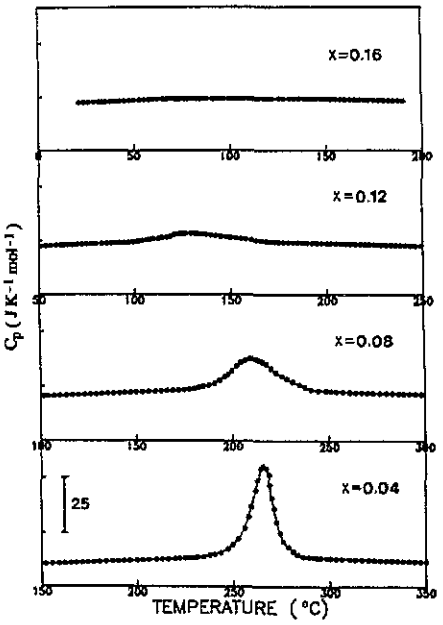

Figure 8. Variation of the heat capacity of the $(Pb_{1-x}Ba_x)(Yb_{1/2}Nb_{1/2})O_3$ system with different Ba concentrations.

peak value becomes weaker such that it is rather difficult to locate the exact transition and determine the entropy associated with it. When possible, the heat of transition and the corresponding entropy change were determined by subtracting the anomalous heat capacity curve from the base line. The heat of transition and entropy change are $\Delta H = 659\ \text{J mol}^{-1}$, $\Delta S = 1.17\ \text{J K}^{-1}\ \text{mol}^{-1}$ for $x = 0.04$ and $\Delta H = 450\ \text{J mol}^{-1}$, $\Delta S = 0.9\ \text{J K}^{-1}\ \text{mol}^{-1}$ for $x = 0.08$.

On the other hand, the heat capacity anomaly associated with phase transition is extremely broadened between $x = 0.1$ and $x = 0.14$. For $x = 0.12$, a very small deviation is seen from the extrapolated base line in the temperature interval 100 to 170 °C as shown in figure 8. This characteristic feature is very similar to the heat capacity manifestation of another DPT ferroelectric $(Pb_{0.7}La_{0.2})(Zr_{0.3}Ti_{0.7})O_3$ reported by Stenger and Burggraaf [15]. The heat and entropy of transition estimated by integrating the area under the anomalous part of the thermal curve are $\Delta H \approx 140\ \text{J mol}^{-1}$ and $\Delta S \approx 0.34\ \text{J K}^{-1}\ \text{mol}^{-1}$. In our study, any distinct heat capacity anomaly near T_t beyond $x = 0.12$ cannot be detected. We suggest the absence of an anomaly as an additional evidence for DPT beyond $x = 0.12$ in our system.

Burggraaf and Stenger [37] have discussed the correlation of ΔS and $\Delta S/T_t$ with the fluctuation probability in conjunction with a small spontaneous lattice deformation and polarization. They have shown that large values of the ratio $\Delta S/T_t$ give sharp transitions, and lower values lead to more diffuse behaviour. The values of ΔH, ΔS and $\Delta S/T_t$ of our system are given in table 1, together with those of some other ferroelectrics for comparison. It is clearly seen that the values of ΔH and ΔS are gradually decreased with increasing Ba concentration for $0 < x < 0.1$, and these values are severely reduced in the DPT region to an unmeasurable extent. Also, the ratio $\Delta S/T_t$ is in line with those of perovskites.

Table 1. Transition enthalpies ΔH and entropies ΔS of $(Pb_{1-x}Ba_x)(Yb_{1/2}Nb_{1/2})O_3$ and some other materials.

Material	Transition temperature T_0 (K)	ΔH (J mol^{-1})	ΔS (J K^{-1} mol^{-1})	$(\Delta S/T_0) \times 10^3$ (J K^{-2} mol^{-1})	Transition	Reference
$PbTiO_3$	763	4830	6.34	8.32	Sharp	[38]
$BaTiO_3$	393	197	0.50	1.26	Sharp	[38]
$Pb(Yb_{1/2}Nb_{1/2})O_3$	581	823	1.42	2.44	Sharp	This work
$(Pb_{0.96}Ba_{0.04})(Yb_{1/2}Nb_{1/2})O_3$	565	659	1.17	2.07	Sharp	This work
$(Pb_{0.92}Ba_{0.08})(Yb_{1/2}Nb_{1/2})O_3$	501	450	0.90	1.79	Sharp	This work
$(Pb_{0.88}Ba_{0.12})(Yb_{1/2}Nb_{1/2})O_3$	413	140	0.34	0.82	Slightly diffuse	This work
PLZT 17/30/70	320	76	0.25	0.71	Slightly diffuse	[24]
PLZT 11.1/55/45	325	46	0.13	0.42	Strongly diffuse	[24]

The broad heat capacity feature of $Sr_{1-x}Ba_xNbO_3$ [2] is rather well established, and it is associated with the dielectric DPT. The extreme broadening in the $(Pb_{1-x}Ba_x)(Yb_{1/2}Nb_{1/2})O_3$ system may well coincide with the dielectric results in the composition range $0.1 < x < 0.14$. Setter and Cross [6] have reported that $Pb(Sc_{1/2}Ta_{1/2})O_3$ with different S, the degree of ordering of the B-site cations (Sc^{3+} and Ta^{3+}), do not show any distinct heat capacity anomaly below $S = 0.5$. Moriya *et al* [39] have shown that no obvious heat capacity anomaly due to the phase transition in the random mixture $Rb_{1-x}(NH_4)_xH_2PO_4$ occurs in the heat capacity curve at $x = 0.74$ and 0.70. In this context, the absence of a heat capacity anomaly beyond $x = 0.14$ can be explained in terms of a non-equilibrium disordered state of the A-site cations (Pb^{2+} and Ba^{2+} ions).

4. Summary

The nature of the phase transitions occurring in the $(Pb_{1-x}Ba_x)(Yb_{1/2}Nb_{1/2})O_3$ $(0 \leq x \leq 0.3)$ ceramics system has been investigated by the dielectric constant, E-P hysteresis loop and heat capacity measurements. It has been found that this pseudo-binary system in the studied composition range can be divided into three physically different regions characterized by the following observed facts.

(i) For $0 \leq x < 0.1$, the AFE–PE phase transition is relatively sharp and the temperature dependence of the dielectric properties is similar to that of pure $Pb(Yb_{1/2}Nb_{1/2})O_3$. The transition temperature T_N steeply decreases with the increasing Ba concentration. Heat capacity measurements have revealed a well-defined anomaly associated with T_N, increasingly broadened with increasing Ba concentration.

(ii) For $0.1 \leq x \leq 0.14$, there have appeared some salient features which are considered to be closely connected with the orthorhombic–pseudo-cubic phase boundary in the vicinity of $x = 0.12$ and the onset of ferroelectricity. The phase transition becomes diffuse and the maximum value of the dielectric constant is abnormally enhanced. The concentration dependence of the transition temperature is also changed. In particular, the heat capacity anomaly is extremely broadened. These features are interpreted in the light of formation of locally ordered dipolar microdomains. Consequently, we suggest that this region is a possible interval of phase coexistence.

(iii) For $0.14 < x \leq 0.3$, the diffuse behaviour of the phase transition is in line with similar observations made on ferroelectric solid solutions showing DPT. The intensity of DPT is gradually strengthened with increasing Ba concentration. The concentration dependence of the transition temperature T_t, defined by the peak dielectric constant, shows a linear-like behaviour. Moreover, we cannot detect any distinct heat capacity anomaly, this is presented as additional evidence of DPT. The absence of an anomaly is explained in terms of a non-equilibrium disordered state of Pb^{2+} and Ba^{2+} ions.

References

[1] Smolensky G A 1970 *J. Phys. Soc. Japan Suppl.* **28** 36
[2] Glass A M 1969 *J. Appl. Phys.* **40** 4699
[3] Fritzberg V Ya 1968 *Sov. Phys.–Solid State* **10** 304
[4] —— 1977 *Bull. Acad. Sci. Latvian SSR* **2** 335
[5] Setter N and Cross L E 1980 *J. Appl. Phys.* **51** 4356
[6] —— 1980 *J. Mater. Sci.* **15** 2478

[7] Burns G 1976 *Phys. Rev.* B **13** 215
[8] Burns G and Dacol F H 1983 *Phys. Rev.* B **28** 2527
[9] Reinecke T L and Ngai K L 1976 *Solid State Commun.* **18** 1543
[10] Darlington C N W 1988 *J. Phys. C: Solid State Phys.* **21** 3851
[11] Salje E and Bismayer U 1989 *J. Phys.: Condens. Matter* **1** 6967
[12] Choo W K and Lee M H 1982 *J. Appl. Phys.* **53** 7355
[13] Yasuda N and Ueda Y 1989 *J. Phys.: Condens. Matter* **1** 497
[14] —— 1989 *J. Phys.: Condens. Matter* **1** 5179
[15] Stenger C G F and Burggraaf A J 1980 *J. Phys. Chem. Solids* **41** 25
[16] Kwon J R and Choo W K 1991 *J. Phys.: Condens. Matter* **3** 2147
[17] Tomashpol'skii Yu Ya and Venevtsev Yu N 1965 *Sov. Phys.–Solid State* **6** 2388
[18] Polyavkov Yu M and Tsyakalov V G 1968 *Sov. Phys.–Solid State* **9** 2600
[19] Kim H J, Park K H and Choo W K 1992 *Ferroelectrics* at press
[20] Uchino K and Nomura S 1982 *Ferroelectrics* **44** 55
[21] Clarke R and Burfoot J C 1974 *Ferroelectrics* **8** 505
[22] Diamond H 1961 *J. Appl. Phys.* **32** 909
[23] Uchino K, Nomura S, Cross L E, Jang S J and Newnham R E 1980 *J. Appl. Phys.* **51** 1142
[24] Jonker G H, Juarez R, Burggraaf A J and Stenger C G F 1980 *Ferroelectrics* **24** 293
[25] Zheludev I S 1971 *Physics of Crystalline Dielectrics* vol 2 *Electrical Properties* (New York–London: Plenum Press) p 363
[26] Migoni R, Bilz H and Bauerle D 1976 *Phys. Rev. Lett.* **35** 1155
[27] Tessman J R, Kahn A H and Shockley W 1953 *Phys. Rev.* **92** 890
[28] Michael K H 1987 *Phys. Rev.* B **35** 1405
[29] Carmesin H O and Binder K 1988 *J. Phys.* A **21** 4053
[30] Höchli U T, Knorr K and Loidl A 1990 *Adv. Phys.* **39** 405
[31] Binder K and Young A P 1986 *Rev. Mod. Phys.* **58** 801
[32] Stachiotti M G and Migoni K L 1990 *J. Phys.: Condens. Matter* **2** 4341
[33] Wang J C 1980 *Phys. Rev.* B **22** 2725
[34] Höchli U T and Maglione M 1989 *J. Phys.: Condens. Matter* **1** 2241
[35] Birge N O, Jeong Y H, Nagel S R, Bhattacharya S and Susman S 1984 *Phys. Rev.* B **30** 2306
[36] Brixel W, Werk M L, Fisher P, Bührer W, Rivera J P, Tissot P and Schmid H 1985 *Japan J. Appl. Phys. Suppl.* **24** 242
[37] Burggraaf A J and Stenger C 1978 *Ferroelectrics* **20** 185
[38] Burfoot J C 1967 *Ferroelectrics* (London: Van Nostrand) p 174
[39] Moriya K, Matsuo T, Suga H and Terauchi H 1985 *Japan J. Appl. Phys. Suppl.* **24** 955